East West University

Summer -2017

Thesis Report

"CIGS solar cell device simulation Silvaco''

Submitted by

Fariha Amin

ID: 2013-2-55-033

&

Tanzia Fairuz

ID: 2013-3-55-020

Thesis Supervisor

Dr. Nahid Aktar Jahan,

Ph.D. Professor Department of Electronics and Communications Engineering

Declaration

We hereby declare that we have completed project on the topic entitled "Enhancement of Conversion Efficiency of CdTe/CIGS   Solar Cell using TCO, Intrinsic and BSF Layers" as well as prepared as research report to the department of Electronics and Communications Engineering, East West University in partial fulfillment of the requirement for the degree of B.Sc. in Electronics and Telecommunications Engineering, under the course "Research/Internship (ETE 498)". We further assert that this report in question is based on our original exertion having never been produced fully and/or partially anywhere for any requirement

Fariha Amin

ID: 2013-2-55-033

&

 Tanzia Fairuz

ID: 2013-3-55-020

Acceptance

This research report presented to the Department of Electronics and Communications Engineering, East West University is submitted in partial fulfillment of the requirement for the degree of B. Sc. In Electronics and Telecommunications Engineering, under complete supervision of the undersigned.

………………………………

Dr. Nahid Aktar Jahan,

Ph.D. Professor Department of Electronics and Communications Engineering

Acknowledgement

Abstract

In this paper, the investigation and optimization of (CIGS)-based solar cells were analyzed and designed by Silvaco-1D software. This paper deals with the influence of a thickness of intrinsic layer, doping density of n-type layer and for different types of TCO layers on the performance of the CIGS-based solar cells. The J-V characteristics and the photovoltaic parameters have been calculated assuming a good optimized structure. Our simulated results exhibit how the absorber and buffer layers thickness, defect density influence the short-circuit current density Isc is 34.235344 , open-circuit voltage Voc is 0.51, fill factor FF is 0.934, and efficiency (η) of solar cell. The optimized solar cell shows an efficiency of 16 % under the AM1.5G spectrum and one sun.

Index

Contents   **Page No**

Chapter 1: Introduction

Chapter 2: Simulation Methodology

Chapter 3: Simulation and result

Chapter 4: Conclusion   32

Chapter 1

Introduction

1.1 Solar Energy

Solar energy is defined as energy obtained from the sun's radiation. The two main forms of solar energy include active solar energy and passive solar energy. Active solar energy involves equipment or an action to convert solar energy into a useful form. One example of active solar energy is the use of solar cells to convert energy from the sun into electrical energy that can be used in the home. Passive solar energy does not require any specific action or equipment. An example of passive solar energy is strategically placing windows in a home to allow sunlight to enter and provide heat [1]. Solar power is the use of the sun energy either directly as thermal energy or through the use of photovoltaic cells in solar panels and transparent photovoltaic glass to generate electricity. Standard photovoltaic solar panels are the most efficient application of photovoltaic. However, photovoltaic glass allows generation from surfaces like building windows that were previously incapable of anything but passive solar energy and also enables other options, like color choices. Other technologies include low-tech solar heaters created from recycled cans that provide an inexpensive source of heat. Concentrated solar power uses multiple lenses or reflectors to collect more of the sun's thermal energy. Thermal energy collected through the day is typically applied to oil or molten salts that retain heat to boil water for steam turbine generators throughout the night. In the data center, solar power and other sources of clean electricity, such as wind power and tidal power, are increasingly implemented to save money, increase self-sufficiency and improve sustainability. Apple, Google and Microsoft are among the major IT companies investing in renewable energy. Besides being cheaper than fossil fuels, solar power avoids the costs associated with environmental damage through extraction, spills and dealing with pollution created through combustion. [2]

1.2 Importance of solar energy

Solar energy is a potential solution to the environmental problems being caused by fossil fuel. When fossil fuels are burned to generate electricity, they release harmful greenhouse gases into the atmosphere. The vast majority of scientists believe that continuing to depend on fossil fuels is going to cause serious environmental problems in the future. Another important use for solar energy is in satellites. Many satellites are engineered with photovoltaic panels, which capture sunlight and convert it into electricity that is used to power the satellite. Solar power is also useful in areas where standard electricity is not available. Emergency phone systems in remote places often use solar power as a dependable power source. Solar energy can also be used to

power devices that run at night. For example, some streetlights are able to charge energy from the sun during the day and then run throughout the night. Solar energy is an important part of life and has been since the beginning of time. Increasingly, man is learning how to harness this important resource and use it to replace traditional energy sources. Plants and animals, alike, use solar energy to produce important nutrients in their cells. Plants use the energy to produce the green chlorophyll that they need to survive, while humans use the sun rays to produce vitamin D in their bodies. However, when man learned to actually convert solar energy into usable energy, it became even more important. [3]

1.3 Generation of Solar Energy

Solar power generating systems absorb sunlight and convert it into electricity that we can use. Every second, the sun sends about 42 trillion kilocalories of energy to the Earth. If we could convert 100% of this solar energy into electricity, we could create one year's worth of power for the entire planet in a single hour. Solar energy is the most powerful of all renewable energy resources. The Earth's reserves of fossil fuels, such as petroleum and coal, may eventually be depleted. Moreover, burning these fossil fuels creates carbon dioxide emissions, which are suspected contributor to climate change. In contrast, as long as the sun exists, we can harness its energy here on Earth. And because solar power emits no carbon dioxide, it is an effective solution to natural resource depletion and climate change problems that are becoming more serious every year.

1.4 Types of Solar Cells

Traditionally there are three types of solar cells:

1. Crystalline Silicon (Polysilicon or monosilicon)

2. Thin film Solar Cell (TFSC)

3. Organic Photovoltaic Cell (OPVC)

Crystalline Silicon (Polysilicon or monosilicon)

This is the first generation PV cell made from silicon. Single crystalline silicon is called monosilicon and the polycrystalline silicon is called polysilicon. Traditionally, monosilicon is used to produce most silicon based microelectronic devices while the ultra-pure polysilicon is used for macro-scale and micro-scale production. Most common application for this is in the semiconductor industry such as integrated circuits and central processing units for computers. Beginning in 2006 ; over half of the world's supply of polysilicon was being used for production

of solar panels. Monosilicon has higher efficiency and thus higher cost. Commercial monosilicon efficiency approximates 22% as produced by US and Japanese solar manufacturers. Crystalline silicon devices have theoretical limiting efficiency of 29% and can achieve an energy payback period of 1-2 years. Most of the low end manufacturers are producing polysilicon PV cells with efficiency of 7-8%.

Thin film Solar Cell (TFSC)

This second generation PV cell applies amorphous, protocrystalline, and nanocrystalline to a plastic or metal surface by chemical vapor deposition. Thin film silicon is opposed to wafer silicon (also called bulk or crystalline silicon). Overall thin film solar cells have lower efficiency and are less expensive than crystalline silicon. Most thin film cell technology has an efficiency of 12-20%, prototype module efficiency of 7-13% and production module efficiency of 9%. State-of-the-art thin film cells can reach the efficiency of 10-16%, with the highest reported efficiency being 18%. Thin film technology has been developed for Building Integrated Photovoltaics (BIPV). These are semitransparent solar cells which can be applied as window glazing so the BIPV technology can be used for window tinting while also generating electricity.

Organic Photovoltaic Cell (OPVC)

This third generation PV cell technology uses organic, electronic conductive polymers or small molecules for light absorption and electrical charge transport. The benefits are low cost and large scale production capability with flexibility. The disadvantages are low efficiency, low stability and low strength compared to traditional non-organic PV cells. For the most part, OPVC technology is still in R&D stages and not ready for mass commercialization. In 2009, about 85% of the PV solar cell market was dominated by crystalline silicon cells while only 15% was represented by thin film solar cells. [4]

1.5 Importance of CdS/CdTe Solar Cell

Second generation thin-film solar cells are the most promising field of photovoltaic solar cell research. They are much cheaper to manufacture due to using simpler deposition processes, and require much less materials as compared to the conventional single-crystal cells. Polycrystalline

CdTe films have high optical absorption coefficient and are normally used in a CdS-CdTe heterojunction configuration. The most important parameter that affects photon absorption is thickness of the CdTe layer. A ZnTe layer is usually used as a back surface barrier to repel the electrons at the CdTe-ZnTe heterojunction and thus decrease the loss of carriers at the back

contact due to presence of a higher band-gap layer at the back. This layer also reduces carrier recombination at the back contact due to the barrier (conduction band discontinuity) for electronsat the interface between CdTe and ZnTe layers. The electrons will reflect at this interface and will be collected with a higher probability at the CdS-CdTe heterojunction. Highly n-type CDS are used as a suitable window layer for these cells. The thickness of CdS affects the cell's conversion efficiency. Up to a certain point, thinner CdS films produce higher short-circuit current densities.

The record cell efficiency of CdTe solar cells were increased by only 1.5% during the last 17 years.Previous groups reported a maximum cell efficiency of 16.5%, but recently, First Solar research group reported a cell efficiency of 20.4% (verified by NREL) and a module efficiency of 13.9% was obtained under the lab conditions.

 Fabrication of high-efficiency CdS-CdTe solar cells with ultra-thin (below 1 m) absorber layers is a challenging yet highly desirable step in improving the cell performance. Thicker absorber layers are generally used to avoid pinholes reaching through to the window layer, which may lead to shorting to the back contact. Typically, the cell performance decreases due to shunting, incomplete absorption, fully depleted CdTe layer, or interference between the main and the back contact junctions when the CdTe layer thickness approaches a certain limit.

Simulation of CdTe thin film solar cells is an important strategy to test the viability of proposed structures and to predict the effect of physical changes on the cell performance. Nowadays, the challenge facing researchers and technologists is how to increase the efficiency of CdS-CdTe solar cells and therefore, decrease the gap between actual efficiency and the theoretical limit. [5] Crystalline silicon solar cells are produced on silicon wafers. It has high conversion efficiency but the availability of Silicon is intricate because of its high cost. Also the fabrication process of the silicon based solar cell is complex. They are not good at high temperature. On the other hand thin films solar are more economical as compared to the crystalline silicon wafer solar cells and also good in cool as well as in high temperature. Crystalline silicon solar cells have light absorbing layers up to 350 μm thick while thin-film solar cells have very thin light absorbing layers generally of the order of 1 μm thickness. Thin films solar have high absorption coefficient. It can occupy both vacuum and non-vacuum process. It is lower cost in comparison of Si based solar cell and also low cost substrate. Current PV module cost for crystalline solar cell is <1.4 USD/W and for CdTe based thin film that is ~0.9 USD/W. PV module size for crystalline solar cell 2 m2 and for CdTe based thin film is 0.72 m2.[6]

1.6 Purpose of This Thesis

The purpose of this thesis is to design and simulate a single junction, five-layer CdS-CdTe solar cell by the use of SILVACO software. The main goal is to create the most efficient and cost effective solar cell by the use of CdS and CdTe materials. In summary, the purpose of this thesis is 1. To design a highly efficient five-layered CdS-CdTe solar cell 2. To optimize the layer thickness and doping density of BSF layer 3. To optimize the layer thickness of intrinsic layer 4. To simulate the whole design using SILVACO software

Chapter 2
Simulation Methodology

The major objectives of numerical modeling and simulation in solar cell research are testing the validity of proposed physical structures, geometry on cell performance and fitting of modeling output to experimental results. Any numerical program capable of solving the basic semiconductor equations could be used for modeling thin film solar cells. This research is physically-based solar cell model using the general-purpose ATLAS device simulator by Silvaco International. Here, the electrical characteristics of a solar cell based on virtual fabrication of its physical structure, allowing for direct manipulation of materials, dimensions, and dopings. In addition, our model has the ability to accurately simulate more advanced solar cell design features including doping gradients, optical properties, back-surface fields, back-surface reflectors, windows, carrier traps, contact grid shading and complex light spectra. Available outputs include efficiency, open circuit voltage, current density, fill factor. The operation of the ATLAS software is described in detail and our model is applied to known single junction cell designs. The results of the solar cell simulation in ATLAS are compared and shown to be similar to published experimental results.

2.1 Models

In our project we used the following models of SILVACO software package models srh conmob fermi ni.fermi bgn optr auger

2.1.1 Shockley-Read-Hall (SRH) Recombination

Phonon transitions occur in the presence of a trap within the forbidden gap of the semiconductor. This is essentially a two-step process, the theory of which was first derived by Shockley and then by Hall. The Shockley-Read-Hall recombination is modeled as follows:

$$R_{SRH} = \frac{pn - n_{ie}^2}{\text{TAUPO}\left[n_{ie}\exp\frac{\text{ETRAP}}{\text{KT}_L}\right] + \text{TAUNO}\left[p + \left(\frac{-\text{ETRAP}}{\text{KT}_L}\right)\right]} \quad \dots\dots\dots\dots\dots\dots\dots\dots\dots\dots\dots [2.1]$$

Where,

ETRAP = The difference between the trap energy level and the intrinsic Fermi level

TL = The lattice temperature in degrees Kelvin

TAUN0 = The electron lifetimes

TAUP0 = The hole lifetimes.

This model is activated by using the SRH parameter of the MODELS statement. The electron and hole lifetime parameters, TAUN0 and TAUP0, are user-definable in the MATERIAL statement. The default values for carrier lifetimes are shown in Table 2.1. Materials other than silicon will have different defaults.

Table2.1 Parameter

Statement	Parameter	Default	Units
MATERIAL	ETRAP	0	eV
MATERIAL	TAUNO	$1 \times 10{-7}$	s
MATERIAL	TAUPO	$1 \times 10{-7}$	s

The constant carrier lifetimes that are used in the SRH recombination model above can be made a function of impurity concentration using the following equation:

$$R_{SRH} = \frac{pn - n_{ie}^2}{\tau_p \left[p + n_{ie} \, exp \left(\frac{ETRAP}{KT_L} \right) \right] + \tau_n \left[p + n_{ie} \, exp \left(\frac{-ETRAP}{KT_L} \right) \right]} \dots\dots\dots\dots\dots\dots\dots\dots\dots\dots\dots\dots\dots 2.2$$

Where,

$$\tau_n = \frac{TAUNO}{AN + BN \left(\frac{N_{total}}{NSRHN} \right) + CN \left(\frac{N_{total}}{NSRHN} \right)^{EN}} \dots\dots\dots\dots\dots\dots\dots\dots\dots\dots\dots\dots 2.3$$

$$\tau_P = \frac{TAUPO}{AP + BP \left(\frac{N_{total}}{NSRHN} \right) + CN \left(\frac{N_{total}}{NSRHN} \right)^{EP}} \dots\dots\dots\dots\dots\dots\dots\dots\dots\dots\dots\dots\dots\dots 2.4$$

Here,

N = The local impurity concentration.

The TAUN0, TAUP0, NSRHN, and NSRHP parameters can be defined on the MATERIAL statement. This model is activated with the CONSRH parameter of the MODELS statement.

Table 2.2 Parameters

Statement	Parameter	Default	Units
MATERIAL	TAUNO	1	s
MATERIAL	NSRHN	-1	cm^{-3}
MATERIAL	TAUPO	1	s
MATERIAL	NSRHP	-1×10^3	cm^{-3}
MATERIAL	AN	1	
MATERIAL	AP	1	
MATERIAL	BN	0	
MATERIAL	BP	1	
MATERIAL	CN	0	
MATERIAL	CP	0	
MATERIAL	EN	0	
MATERIAL	EP	0	

2.1.2 Concentration Dependent Mobility (CONMOB)

CONMOB specifies that a concentration dependent mobility model be used for silicon and gallium arsenide. This model is a doping versus mobility table valid for 300K only.

2.1.3 Fermi-Dirac (FERMI)

Fermi-Dirac reduced carrier concentrations in heavily doped regions. Electrons in thermal equilibrium at temperature TL with a semiconductor lattice obey Fermi-Dirac statistics. That is the probability $f(\varepsilon)$ that an available electron state with energy ε is occupied by an electron is:

$$f(\varepsilon) = \frac{1}{1 + \exp\left(\frac{\varepsilon - E_F}{KT_L}\right)} \quad \text{...[2.4]}$$

Where,

EF = A spatially independent reference energy known as the Fermi level
k = is Boltzmann's constant. If $\varepsilon - E$
F>>kTL, then the above equation can be express as,

$$f(\varepsilon) = \exp\frac{\varepsilon - E_F}{KT_L}$$

NI.FERMI includes the effects of Fermi statistics into the calculation of the intrinsic concentration in expressions for SRH recombination.

2.1.4 Bandgap Narrowing (BGN)

In the presence of heavy doping, greater than 1018cm-3, experimental work has shown that the pn product in silicon becomes doping dependent. As the doping level increases, a decrease in the bandgap separation occurs, where the conduction band is lowered by approximately the same amount as the valence band is raised. In ATLAS this is simulated by a spatially varying intrinsic concentration nie defined according to equation

$$n_{ie}^2 = n_i^2 \exp\frac{\Delta Eg}{kt} \dots\dots\dots\dots\dots\dots\dots\dots\dots\dots\dots\dots\dots\dots\dots\dots\dots\dots\dots.2.6$$

Bandgap narrowing effects in ATLAS are enabled by specifying the BGN parameter of the MODELS statement. These effects may be described by an analytic expression relating to the variation in bandgap, ΔEg, to the doping concentration, N. The expression used in ATLAS is from Slotboom and de Graaf

$$\Delta Eg = BGN.E\{ln \frac{N}{BGN.N} + [(ln \frac{N}{BGN.N}^2)2 + BGN.C]^{\frac{1}{2}}\} \dots\dots\dots\dots\dots\dots\dots..[2.7]$$

We can specify the BGN.E, BGN.N, and BGN.C parameters in the MATERIAL statement. The default values from Slotboom and Klaassen are shown in Table 2.3. The Klaassen defaults will be used if you specify the BGN.KLA parameter in the MODELS statement. Otherwise, the Slotboom values will be used (by default). You can select a second set of defaults by specifying BGN.KLASSEN.

Table 2.3

Parameters for Bandgap Narrowing Model

Statement	parameter	values	units
MATERIAL	BGN.E	0.009	eV
MATERIAL	BGN.N	$1\times10_{17}$	cm^{-3}
MATERIAL	BGN.C	0.5	-

2.1.5 Optical Generation/Radiative Recombination

OPTR selects the optical recombination model. When this parameter is specified, the COPT parameter of the MATERIAL statement should be specified. The next physical mechanisms we have to consider for generation/recombination are photon transition. This mechanism occurs primarily in one step and is therefore a direct generation/recombination mechanism. There are two partial processes involved. For radiative recombination, an electron loses energy on the order of the band gap and moves from the conduction band to the valence band. For optical generation, an electron moves from the valence band to the conduction. In silicon, band to band generation/recombination is insignificant. This effect, however, is important for narrow gap semiconductors and semiconductors whose specific band structure allows direct transitions. By assuming a capture rate CcOPT and an emission rate CeOTP, the involved partial processes can be written as

$$R \text{ np OPT} = C_C^{OPT\,NP} \dots \dots \dots \dots \dots \dots \dots \dots \dots \dots \dots \dots \dots [2.8]$$

for recombination and GnpOPT = CeOPT………………………………………… [2.9]

for gneration These rates must be equal in thermal equilibrium so that
$$\text{CnpOPT} = C_C^{OPT}(np - n_{ie}^2)$$
……………………………………………………………………………………...[2.10]

 The total band to band generation/recombination is the difference of the partial rates, which equates to
RnpOPT = CcOPT (np-
n2ie)……………………………………………………………………. [2.11]

In ATLAS, COPT is used express CcOPT and can be defined away from default values on the materials statement or implemented using a C-Interpreter routine. To turn on the optical recombination/ generation model, define the OPTR keyword on the MODELS statement.

2.1.6 Auger Recombination

 Auger is the Direct Recombination Model. Auger recombination occurs through a three particle transition whereby a mobile carrier is either captured or emitted. It is important at high current densities. The underlying physics for such processes is unclear and normally a more qualitative understanding is sufficient. Auger Recombination is commonly modeled using the expression:

$$R_{Auger} = \text{AUGN } (pn^2 - nn_{ie}^2) + \text{AUGP } (np^2 - -pn_{ie}^2 \text{..}) \quad [2.12]$$

Where the model parameters AUGN and AUGP are user-definable in the MATERIAL statement. We can activate this model with the AUGER parameter from the MODELS statement

Table2.4   Parameters for Equation [2.12]

Statement	Parameter	Value	Units
MATERIAL	AUGN	0	ccm^6/s
MATERIAL	AUGP	0	cm^6/s

.

U.AUGER   specifies that the integrated Auger recombination rate is to be extracted.

2.2 Simulating Photodetectors

This section describes techniques simulate photodetectors. This section applies to the simulation of the following devices: p-n and p-i-n photodiodes, avalanche photodiodes, Schottky photodetectors, CCDs, MSMs, photoconductors, optical FETs and optically triggered power devices.

2.2.1 Defining Optical Sources

We can define up to ten optical sources. Optical sources are described by using the BEAM statement. All BEAM statements must appear somewhere after the MESH, REGION, DOPING, and ELECTRODE statements and before any SOLVE statement. The parameters in the BEAM statement describe a single optical source. The NUM parameter is used to uniquely identify one optical source. Values between 1 and 10 are valid for the NUM parameter. Optical sources are subsequently referred to by the value of their NUM parameter. The power of the optical beam is set by using the B<n> parameter of the SOLVE statement, where n is the beam number defined by NUM. The ANGLE parameter specifies the angle of the direction of propagation of the beam with respect to the device coordinate system. ANGLE=90 specifies vertical (normal) illumination from above. The optical source can be either monochromatic or multispectral. For monochromatic sources, we can use the WAVELENGTH parameter to assign the optical wavelength. WAVELENGTH uses the unit microns to be more consistent with the rest of ATLAS. For multispectral sources, spectral intensity is described in an external ASCII file indicated by the POWER.FILE parameter. This is a text file that contains a list of pairs defining wavelength and spectral intensity. The first line of the file gives the integer number of wavelength-intensity pairs in the file. An example of such a file is shown below.

4

0.4 0.5

0.5 1.0

0.6 1.2

0.7 1.1

This example specifies that there are four samples and that at a wavelength of 0.4 μm, the intensity is 0.5 Watts per square cm per μm of wavelength, and so on. With multispectral sources, specify a discretization of the interpolated information. Values must be specified for the WAVEL.START, WAVEL.END, and WAVEL.NUM parameters. These values specify the starting and ending wavelengths and the number of wavelengths to sample. LUMINOUS uses wavelengths at equal intervals over a specified range of wavelengths. If we don't specify the values of WAVEL.START, WAVEL.END, and WAVEL.NUM, these parameters take on the corresponding values from the specified POWER.FILE. For the example file shown above, LUMINOUS uses the following default values of these parameters: WAVEL.START=0.4, WAVEL.END=0.7, and WAVEL.NUM=4. LUMINOUS performs an independent ray trace at each of the sample wavelengths. For example: WAVEL.START=0.4 WAVEL.END=0.6 WAVEL.NUM=2 causes ray traces at wavelengths of 0.45 and 0.55. LUMINOUS obtains the intensity associated with each sample by integrating the values of the spectral intensity file using a piece wise linear approximation. Each integral is performed over the range between successive midpoints. In the preceding example, the integration for the sample at 0.45 would be performed over the range of 0.4 to 0.5. For a multispectral source, the generation rate is given by:

$$G = \eta_0 \int_{WAVEL.END}^{WAVEL.END}$$

$$\frac{P(\lambda)L\lambda}{hc} \alpha e^{-\alpha Y} d\lambda$$

$$\int_{WAVEL.START} \alpha e^{-\alpha y} d\lambda \cdots\cdots\cdots\cdots\cdots\cdots\cdots\cdots\cdots\cdots\cdots\cdots\cdots [2.13]$$

Where,

η_0 = The internal quantum efficiency.

$P(\lambda)$ = The power spectral density of the source.

L = A factor representing the cumulative loss due to reflections, transmissions, and absorption over the ray path.

λ = The wavelength.

 h = Planck's constant

c = The speed of light.

α = The absorption coefficient

 y = The depth of the device, where x,y forms the two-dimensional mesh.

 WAVEL.START= The starting of spectral limits specified on the BEAM statement

WAVEL.END = The ending of spectral limits specified on the BEAM statement.

The source photocurrent is given by:

$$IS = q\frac{bn}{hc} \int_{wavel\ .end}^{wavel\ .start} P(\lambda)\lambda d\lambda \quad \dots\dots\dots\dots\dots\dots\dots\dots\dots\dots\dots\dots\dots\dots\dots\dots.2.14$$

Where,

P(λ) = The power spectral density of the source.

The other parameters have the same definition as in Equation The available photo current is given by:

$$IA = q\frac{bn}{hc} \sum Nr\ _{i=1} Wr \int_{0}^{xi} \int_{wavel\ .start}^{wavel\ .end} P(\lambda)\ \alpha ie - \alpha i y\ Pi\ dy d\lambda \quad \dots\dots\dots\dots\dots\dots..2.15$$

where,

P(λ) = The power spectral density of the source.

 The other parameters have the same definition as in Equation. LUMINOUS allows you to choose the units of spectral intensity in an input spectrum file. By default, the units of spectral intensity in the POWER.FILE are W/cm2. In this case, LUMINOUS carries out the integration. If the units of spectral intensity in the POWER.FILE are W/cm2, then you need to use the flag INTEGRATE on the BEAM statement. In this case, each value P(λ) in the second column of the file is a total intensity for a corresponding spectral interval. Integrals

over spectrum are reduced to summations of P(λ) values. In both c subsequently specified value of Bn on the SOLVE statement as a unit less multiplier or scale factor for intensity. This is different from monochromatic case where this parameter has units of W/cm2. To preserve

consistency with monochromatic case, you can also do the same in the multispectral applications. If you specify the total beam intensity for multispectral sources using Bn parameter on the SOLVE statement, you need to set NORMALIZE flag on the BEAM statements. This ensures that the intensity spectrum is normalized and Bn has units of W/cm^2

One of the simpler tasks in characterizing a photodetector design is to measure DC detection efficiency. This will be done typically as a function of bias voltage, optical intensity, or wavelength. Each of these analyses can be performed using the SOLVE statement. The Bn parameter can be used to set the optical intensity of the optical sources described in the previous section. The following example illustrates obtaining a solution with a specified optical intensity:

SOLVE B1=1.0

This specifies that a solution is to be obtained for an optical intensity in the beam numbered "1" of 1.0 Watt/cm^2. If this were the first SOLVE statement specified, the ray trace in LUMINOUS would be initiated.

At the start of the solution, the optical intensities of each optical source with a positive intensity is printed. In addition, the available photocurrent and source photocurrent are printed. The available photocurrent divided by the source photocurrent is a measure of the external quantum efficiency of the detector. The calculated terminal current can be divided by the source or available photocurrents is used to evaluate the internal quantum efficiency of the device. To obtain VOC and ISC for a solar cell, first define the illumination conditions. This should be done as discussed above in describing multi-spectral sources. The short circuit current is obtained by defining the contacts as voltage dependent contacts (default) and obtaining a solution with the device under zero bias with illumination. This can typically be done as a first step by the following input statement, for example:

SOLVE B1=1

In this statement, it's assumed the source, B1, has been already defined and the intensity is expected in the actual device. When you obtain a solution, the terminal currents represent the short circuit current.The open circuit voltage is obtained by defining one or more of the contacts as current controlled. This is done using the CONTACT statement. For example: CONTACT NAME=anode CURRENT defines that electrode number 1 is a current controlled electrode. The response of photodetectors to angle of incidence can be obtained in a manner analogous to the method used to obtain spectral response. In this case, the ANGLE parameter of the SOLVE statement specifies an angle added to the value of the BEAM parameter PHI (ANGLE). This allows collection of response versus angle. The following examples statements demonstrate the

syntax. SOLVE B1=1 ANGLE=0 SOLVE B1=1 ANGLE=10 SOLVE B1=1 ANGLE=20 SOLVE B1=1 ANGLE=30 SOLVE B1=1 ANGLE=40 SOLVE B1=1 ANGLE=50 SOLVE B1=1 ANGLE=60 Equivalently, you may find it more convenient to specify an angle ramp. To specify a ramp of angle, you should assign the BEAM parameter to the beam index of the optical source to be ramped. Also, you should specify the initial angle with the ANGLE parameter, the final angle with the AFINAL parameter, and the angle step size with the ASTEP parameter as illustrated in the following.

 SOLVE B1=1 BEAM=1 ANGLE=0.0 ASTEP=10.0 AFINAL=60.0

 This is completely analogous to the seven statements described above.

Equivalently, you may find it more convenient to specify an angle ramp. To specify a ramp of angle, you should assign the BEAM parameter to the beam index of the optical source to be ramped. Also, you should specify the initial angle with the ANGLE parameter, the final angle with the AFINAL parameter, and the angle step size with the ASTEP parameter as illustrated in the following.

 SOLVE B1=1

BEAM=1

 ANGLE=0.0

 ASTEP=10.0

 AFINAL=60.0

 This is completely analogous to the seven statements described above.

Luminous 2D provide flexible means for defining multispectral sources. In addition, you can directly access built-in public domain solar spectra for am0 and am1.5 conditions by specifying AM0 or AM1.5 on the BEAM statement. These spectra consist of numerous samples. The following is an example of how you might define the BEAM statement for analysis of am1.5 conditions with subsampling. BEAM NUM=1 AM1.5 WAVEL.START=0.3 WAVEL.END=1.0 WAVEL.NUM=50 Here, we are choosing to simulate am1.5 conditions sampled between 0.3 microns and 1.0 microns at 50 samples. We do not have to worry about sampling the many peaks and valleys in the solar spectrum as it is automatically integrated into each subsample. The subsampling effects only the number of wavelengths for which the propagation model is calculated not the integrated intensity. Ray tracing is the principal propagation model for cases where we are not concerned about interference or diffraction effects in the bulk of the device. This is most useful for relatively thick bulk devices, such as crystalline silicon devices. It is useful for planar or textured devices. For textured devices, the texturing must be described

explicitly in the device structure. The following gives an example of the specification of ray tracing for the optical propagation model for Luminous.

BEAM NUM=1 AM1.5 WAVEL.START=0.3 WAVEL.END=1.0 WAVEL.NUM=50

In this case, we will perform 50 ray traces. The omission of other model keywords, such as TR.MATRIX, FDTD, or BPM, signifies that ray tracing will be performed. For Luminous, the algorithm automatically traces exactly the right number of rays to completely resolve all discontinuities at the surface and deep into the device. Here, we will describe how to extract the most common figures of merit for solar cells. These extraction methods are solution strategies placed in your input deck after defining the device structure, physical models, and the optical source as described in the previous section. Typically, the first step in solar analysis is to illuminate the device. You can turn on the illumination by assigning the beam intensity on a SOLVE statement as follows:

SOLVE B1=1.0

 Here, we assign a value of one "sun" to the intensity of the optical source indexed as number

 1" (B1).

As we had assigned AM1.5 on the BEAM statement, this corresponds to standard test conditions. In some cases, we may encounter convergence difficulties and may need to ramp the light intensity as shown in the following:

 SOLVE B1=1.0

 You may also choose to assign the beam intensity to a value greater than one to simulate solar concentrator effects. Since we have not yet assigned any bias voltages, the current in the run time output corresponds to the short circuit current (Isc).


2.2.2 Air mass

The Air Mass is the path length which light takes through the atmosphere normalized to the shortest possible path length (that is, when the sun is directly overhead). The Air Mass quantifies the reduction in the power of light as it passes through the atmosphere and is absorbed by air and dust.

The Air Mass is defined as:
$AM = 1$
$cos(q)$ [2.16] Where, q= The angle from the vertical (zenith angle). When the sun is directly overhead, the air mass is 1
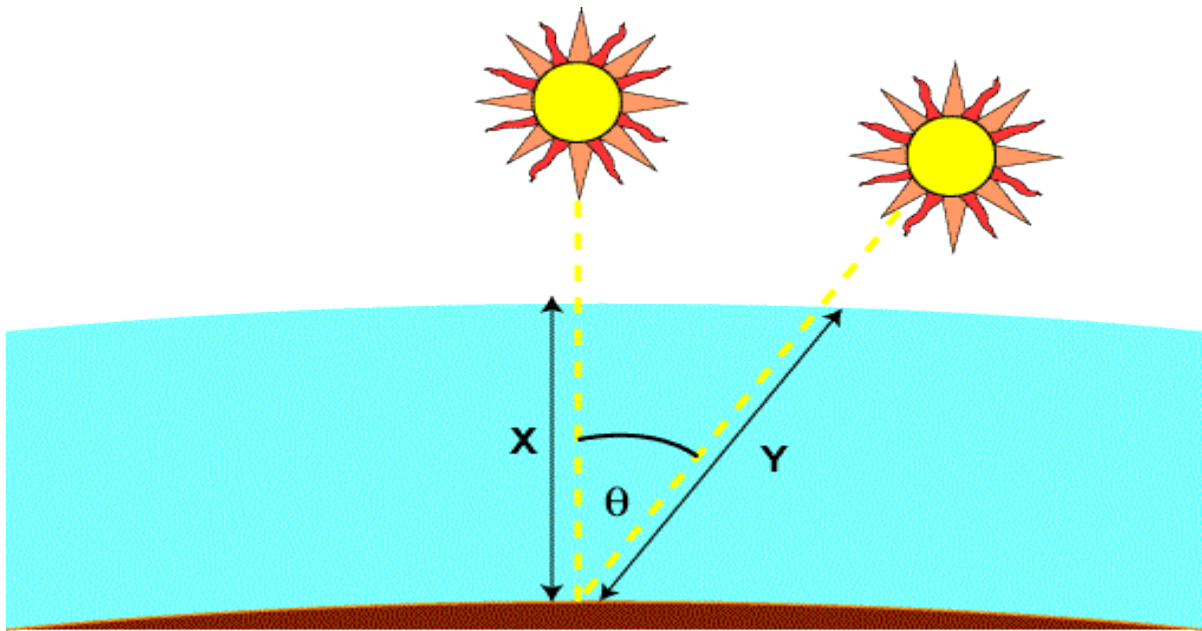
The air mass represents the proportion of atmosphere that the light must pass through before striking the Earth relative to its overhead path length, and is equal to Y/X. An easy method to determine the air mass is from the shadow of a vertical pole
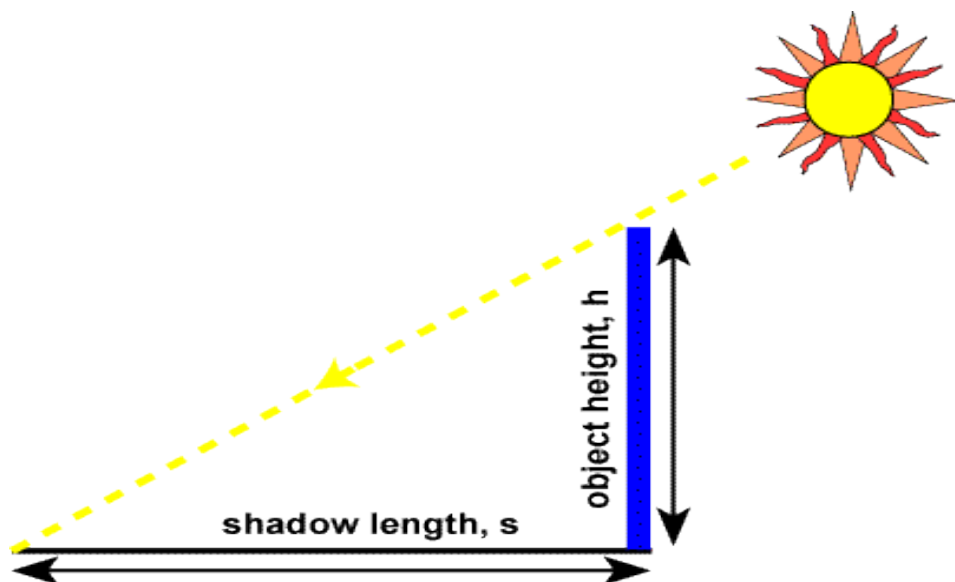
Air mass is the length of the hypotenuse divided by the object height h, and from Pythagoras's theorem we get:

$$AM = \sqrt{1+\left(\frac{s}{h}\right)^2} \quad \cdots\cdots\cdots\cdots\cdots\cdots\cdots\cdots\cdots\cdots\cdots\cdots\cdots\cdots\cdots\cdots\cdots\cdots\cdots\cdots (2.17)$$

The above calculation for air mass assumes that the atmosphere is a flat horizontal layer, but because of the curvature of the atmosphere, the air mass is not quite equal to the atmospheric path length when the sun is close to the horizon. At sunrise, the angle of the sun from the vertical position is 90° and the air mass is infinite, whereas the path length clearly is not. An equation which incorporates the curvature of the earth is:

$$AM = \frac{1}{\cos q + 0.50572\,(96.07995 - q)^{-1.6364}}$$

The efficiency of a solar cell is sensitive to variations in both the power and the spectrum of the incident light. To facilitate an accurate comparison between solar cells measured at different times and locations, a standard spectrum and power density has been defined for both radiation outside the Earth's atmosphere and at the Earth's surface. The standard spectrum at the Earth's surface is called AM1.5.The intensity of AM1.5 radiation can be approximated by reducing the AM0 spectrum by 28% (18% due to absorption and 10% to scattering). The global spectrum is 10% higher than the direct spectrum. These calculations give approximately 970 W/m2 for AM1.5G. However, the standard AM1.5G spectrum has been normalized to give 1kW/m2 due to the convenience of the round number and the fact that there are inherently variations in incident solar radiation. The standard spectrum is listed in the Appendix page. The standard spectrum outside the Earth's atmosphere is called AM0, because at no stage does the light pass through the atmosphere. This spectrum is typically used to predict the expected performance of cells in space

Silvaco code :

```
go atlas

mesh

x.mesh location = 0 spacing = 0.1

x.mesh location = 3 spacing = 0.1
```

x.mesh location = 3.5 spacing = 0.1

y.mesh location = 0 spacing = 0.01

y.mesh location = 0.05 spacing = 0.01

y.mesh location = 0.25 spacing = 0.01

y.mesh location = 1 spacing = 0.01

y.mesh location = 1.2 spacing = 0.01

y.mesh location = 1.4 spacing = 0.01

y.mesh location = 1.6 spacing = 0.01

y.mesh location = 1.8 spacing = 0.01

y.mesh location = 2 spacing = 0.01

y.mesh location = 2.2 spacing = 0.01

y.mesh location = 2.4 spacing = 0.01

y.mesh location = 2.6 spacing = 0.01

y.mesh location = 2.8 spacing = 0.01

y.mesh location = 3 spacing = 0.01

y.mesh location = 3.05 spacing = 0.01

region num = 1 x.min = 0 x.max = 3   y.min = 0   y.max = 0.05 material = ZnO

region num = 2 x.min = 3 x.max = 3.5 y.min = 0   y.max = 0.05 material = aluminum

region num = 3 x.min = 0 x.max = 3.5 y.min = 0.05 y.max = 0.25 material = ZnO

region num = 4 x.min = 0 x.max = 3.5 y.min = 0.25 y.max = 1   material = CdS

region num = 5 x.min = 0 x.max = 3.5 y.min = 1   y.max = 1.2 material = CIGS

region num = 6 x.min = 0 x.max = 3.5 y.min = 1.2 y.max = 1.4 material = CIGS

region num = 7 x.min = 0 x.max = 3.5 y.min = 1.4 y.max = 1.6 material = CIGS

region num = 8 x.min = 0 x.max = 3.5 y.min = 1.6 y.max = 1.8 material = CIGS

region num = 9 x.min = 0 x.max = 3.5 y.min = 1.8 y.max = 2   material = CIGS

region num = 10 x.min = 0 x.max = 3.5 y.min = 2   y.max = 2.2 material = CIGS

region num = 11 x.min = 0 x.max = 3.5 y.min = 2.2 y.max = 2.4 material = CIGS

region num = 12 x.min = 0 x.max = 3.5 y.min = 2.4 y.max = 2.6 material = CIGS

region num = 13 x.min = 0 x.max = 3.5 y.min = 2.6 y.max = 2.8 material = CIGS

region num = 14 x.min = 0 x.max = 3.5 y.min = 2.8 y.max = 3   material = CIGS

region num = 15 x.min = 0 x.max = 3.5 y.min = 3   y.max = 3.05 material = Molibdinum

electrode x.min = 3 x.max = 3.5 y.min = 0   y.max = 0.05 material = aluminum name = cathode

electrode x.min = 0 x.max = 3.5 y.min = 3 y.max = 3.05 material = Molibdinum name = anode

doping x.min = 0 x.max = 3.5 y.min = 0.05 y.max = 0.25 uniform n.type concentration=1e18

doping x.min = 0 x.max = 3.5 y.min = 0.25 y.max = 1   uniform n.type concentration=1.1e18

doping x.min = 0 x.max = 3.5 y.min = 1   y.max = 1.2 uniform p.type concentration=2e16

doping x.min = 0 x.max = 3.5 y.min = 1.2 y.max = 1.4 uniform p.type concentration=2e16

doping x.min = 0 x.max = 3.5 y.min = 1.4 y.max = 1.6 uniform p.type concentration=2e16

doping x.min = 0 x.max = 3.5 y.min = 1.6 y.max = 1.8 uniform p.type concentration=2e16

doping x.min = 0 x.max = 3.5 y.min = 1.8 y.max = 2   uniform p.type concentration=2e16

doping x.min = 0 x.max = 3.5 y.min = 2   y.max = 2.2 uniform p.type concentration=2e16

doping x.min = 0 x.max = 3.5 y.min = 2.2 y.max = 2.4 uniform p.type concentration=2e16

doping x.min = 0 x.max = 3.5 y.min = 2.4 y.max = 2.6 uniform p.type concentration=2e16

doping x.min = 0 x.max = 3.5 y.min = 2.6 y.max = 2.8 uniform p.type concentration=2e16

doping x.min = 0 x.max = 3.5 y.min = 2.8 y.max = 3   uniform p.type concentration=2e16

material TAUN=1e-7 TAUP=1e-7 COPT=1.5e-10 AUGN=8.3e-32 AUGP=1.8e-31

#material material=ZnO   AFFINITY=4.50 EG300=3.30 PERMITTIVITY=9.00 MUN= 50 MUP= 5 NC300= 2.2e18 NV300= 1.8e19 RESISTIVITY= 480

ZnO

material material=ZnO EG300=3.3 PERMITTIVITY=9 AFFINITY=4.7 MUN=100 MUP=25 NC300=2.2e18 NV300=1.8e19

Cds

material material=CdS EG300=2.4 PERMITTIVITY=10 AFFINITY=4.5 MUN=100 MUP=25 NC300=2.2e18 NV300=1.8e19

CIGS

material material=molibdinum resistivity=120

struct outfile=CIGS_Solar_1.str

tonyplot CIGS_Solar_1.str

models srh fermi ni.fermi conmob optr auger bgn print

SOLVING I-V CURVE

BEAM NUM=1 AM1.5 WAVEL.START=0.3 WAVEL.END=1.2 WAVEL.NUM=50

SOLVE B1=1 BEAM=1 ANGLE=0.0 ASTEP=10.0 AFINAL=60.0

LOG OUTFILE="CIGS_Solar_1.LOG"

SOLVE VANODE=0 NAME=ANODE VSTEP=0.001 VFINAL=1

TONYPLOT CIGS_Solar_1.LOG

quit

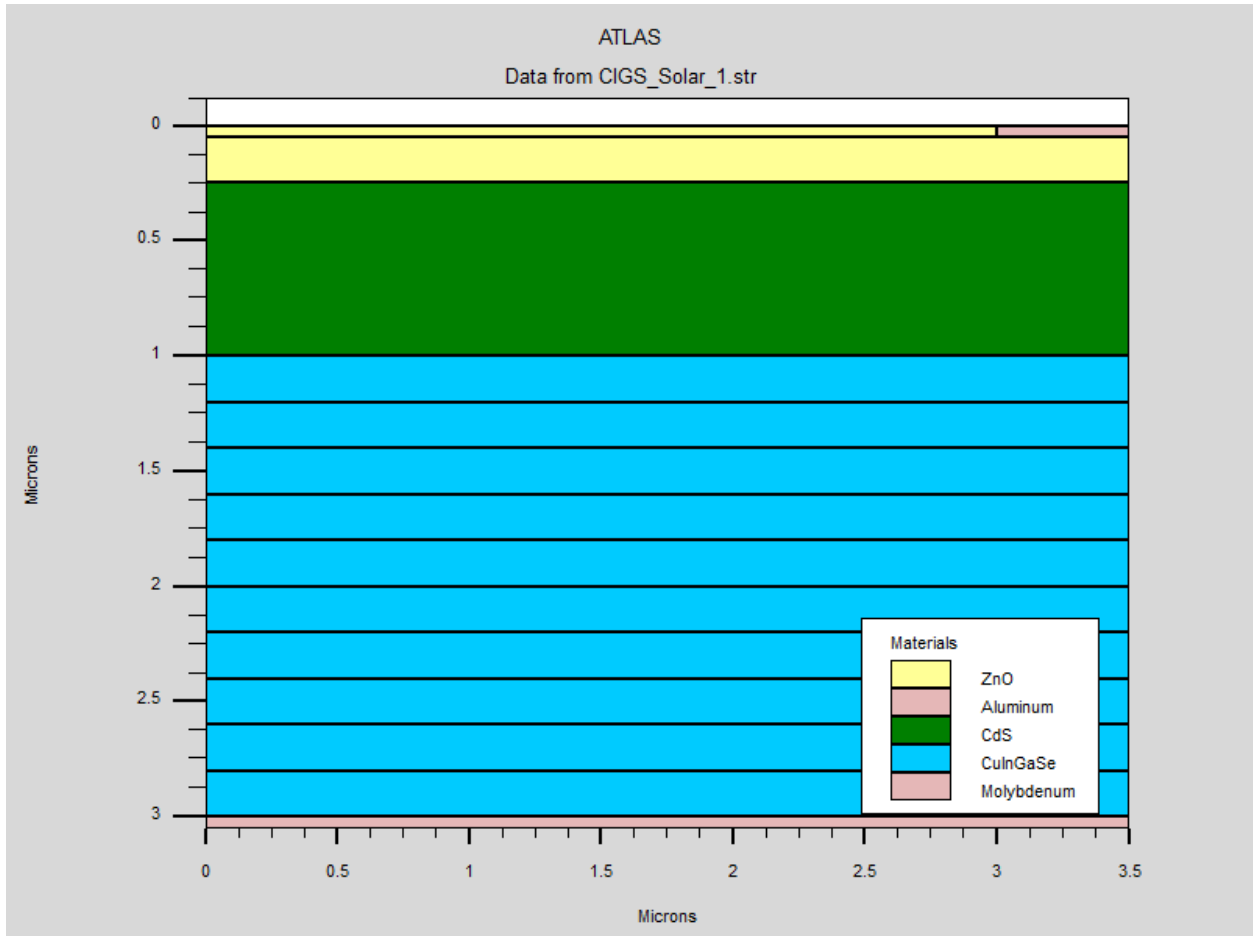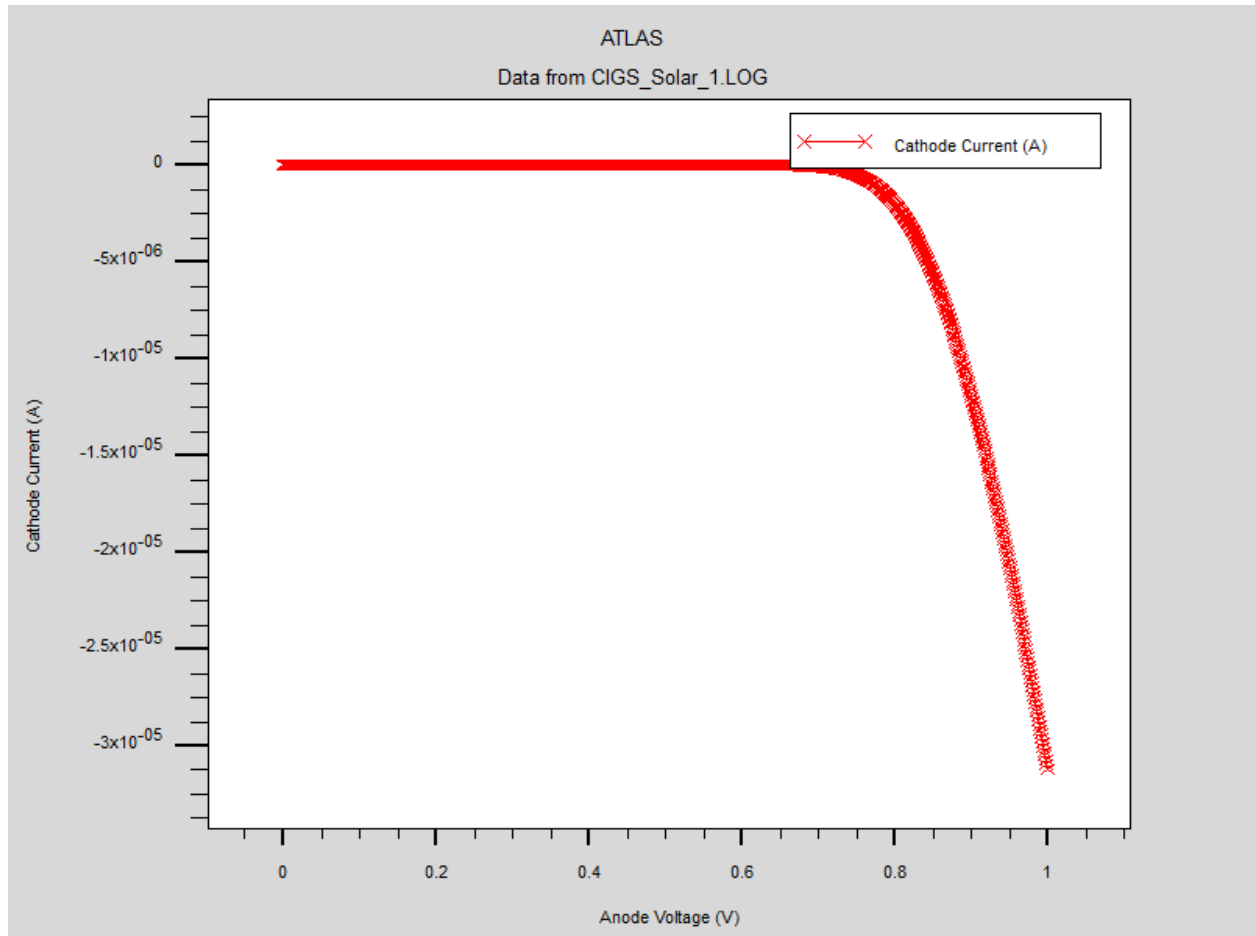# Chapter 3
Simulated Results

3.1 Proposed Solar Cell

figure -3.1: Proposed CdTe-CiGs Solar Cell

ATLAS
Data from CIGS_Solar_1.LOG

3.2 TCO Layer:

Transparent conductive oxides (TCO) are doped metal oxides used in optoelectronic devices such as flat panel displays and photovoltaics (including inorganic devices, organic devices, and dyesensitized solar cell). Most of these films are fabricated with polycrystalline or amorphous microstructures. Typically, these applications use electrode materials that have greater than 80% transmittance of incident light as well as electrical conductivities higher than 103 S/cm for efficient carrier transport. In general, TCOs for use as thin-film electrodes in solar cells should have a minimum carrier concentration on the order of 1020 cm-3 for low resistivity and a bandgap greater than 3.2 eV to avoid absorption of light over most of the solar spectra. Mobility in these films is typically limited by ionized impurity scattering due to the large amount of ionized donors in the and is on the order of 40 cm2/(V·s) for the best performing TCOs. Current transparent conducting oxides used in industry are primarily n-type conductors, meaning their primary conduction is as donors of electrons. This is because electron motilities are typically

higher than hole motilities, and the difficulty of finding shallow acceptors in wide band gap oxides to create a large hole population. Suitable p-type transparent conducting oxides are still being researched, though the best of them are still orders of magnitude behind n-type TCOs. To date, the industry standard in TCOs is ITO, or tin-doped indium-oxide. This material boasts a low resistivity of ~10^{-4} $\Omega \cdot$cm and a transmittance of greater than 80%. ITO has the drawback of being expensive. Indium, the film's primary metal, is rare (6000 metric tons worldwide in 2006), 27 and its price fluctuates due to market demand (over \$800 per kg in 2006). For this reason, doped binary compounds such as aluminum-doped zinc-oxide (AZO) and indium-doped cadmium-oxide have been proposed as alternative materials. AZO is composed of aluminum and zinc, two common and inexpensive materials, while indium-doped cadmium oxide only uses indium in low concentrations. Other novel transparent conducting oxides include barium stannite and the correlated metal oxides strontium vanadate and calcium vanadate. Binary compounds of metal oxides without any intentional impurity doping have also been developed for use as TCOs. These systems are typically n-type with a carrier concentration on the order of 10^{20} cm-3, provided by interstitial metal ions and oxygen vacancies which both act as donors. However, these simple TCOs have not found practical use due to the high dependence of their electrical properties on temperature and oxygen partial pressure.

3.3 BSF Layer

An effect is employed at the rear surface to minimize the impact of rear surface recombination velocity on voltage and current if the rear surface is closer than a diffusion length to the junction. A "back surface field" (BSF) consists of a higher doped region at the rear surface of the solar cell. The interface between the high and low doped regions behaves like a p-n junction and an electric field forms at the interface which introduces a barrier to minority carrier flow to the rear surface. The minority carrier concentration is thus maintained at higher levels in the bulk of the device and the BSF has a net effect of passivating the rear surface.

3.4 Intrinsic Layer

PIN photodiodes are used in fiber optic network cards and switches. As a photo detector, the PIN diode is reverse biased. Under reverse bias, the diode ordinarily does not conduct (save a small dark current or leakage). When a photon of sufficient energy enters the depletion region of the diode, it creates an electron-hole pair. The reverse bias field sweeps the carriers out of the region creating a current. Some detectors can use avalanche multiplication. The same mechanism applies to the PIN structure, or p-i-n junction, of a solar cell. In this case, the advantage of using a PIN structure over conventional semiconductor p–n junction is the better long wavelength response of the former. In case of long wavelength irradiation, photons penetrate deep into the

cell. But only those electron-hole pairs generated in and near the depletion region contribute to current generation. The depletion region of a PIN structure extends across the intrinsic region, deep into the device. This wider depletion width enables electron-hole pair generation deep within the device. This increases the quantum efficiency of the cell.
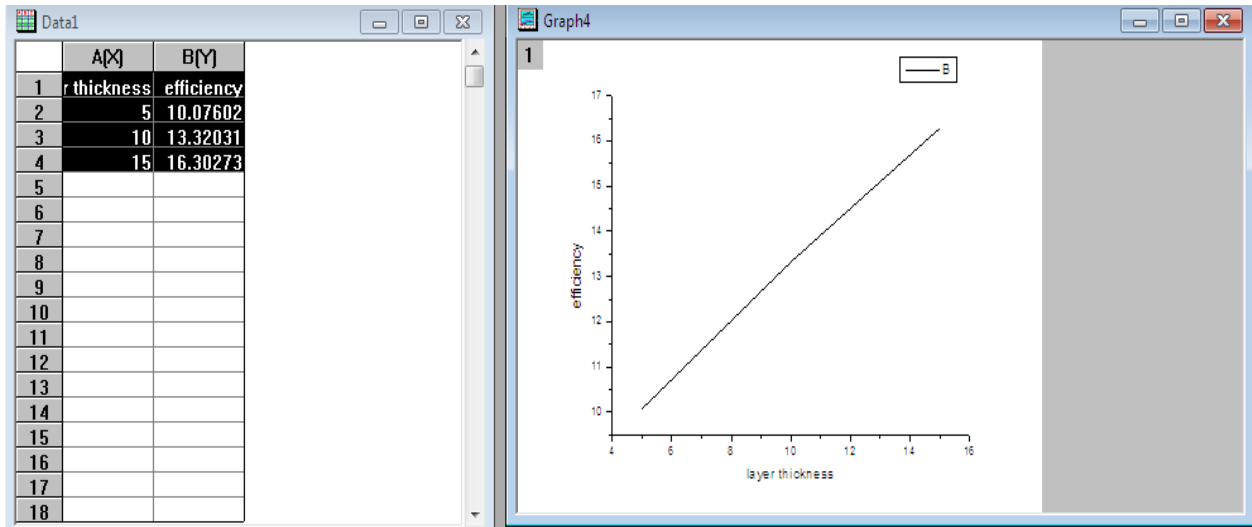

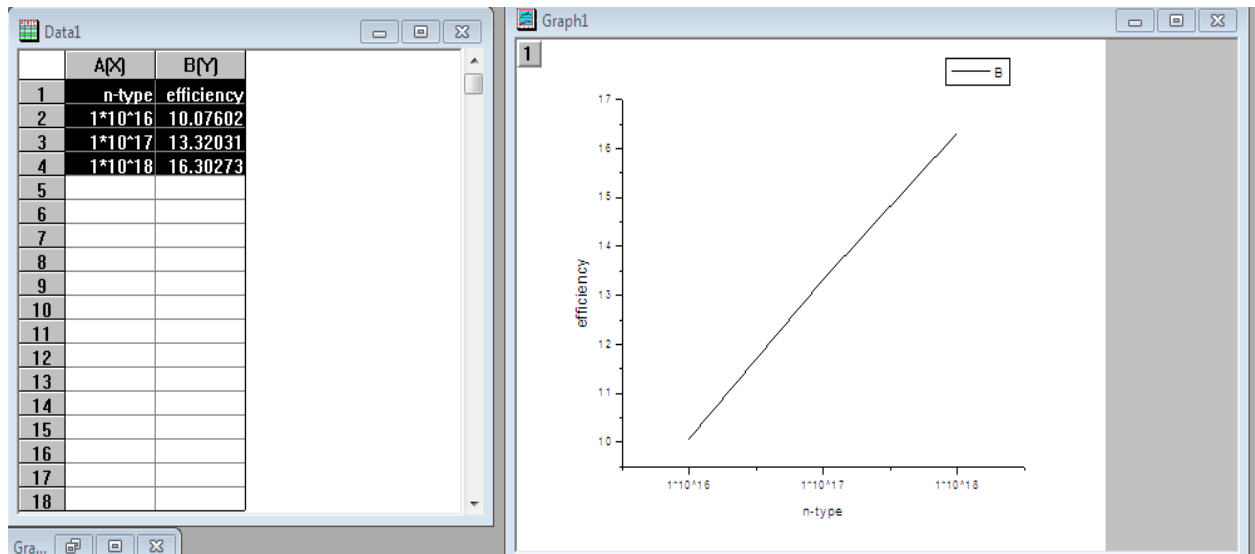|	A[X]	B[Y]
1	r thickness	efficiency
2	5	10.07602
3	10	13.32031
4	15	16.30273
5		
6		
7		
8		
9		
10		
11		
12		
13		
14		
15		
16		
17		
18		

Fig: thickness vs efficiency

	A[X]	B[Y]
1	n-type	efficiency
2	1*10^16	10.07602
3	1*10^17	13.32031
4	1*10^18	16.30273
5		
6		
7		
8		
9		
10		
11		
12		
13		
14		
15		
16		
17		
18		

Fig: n-type vs efficiency

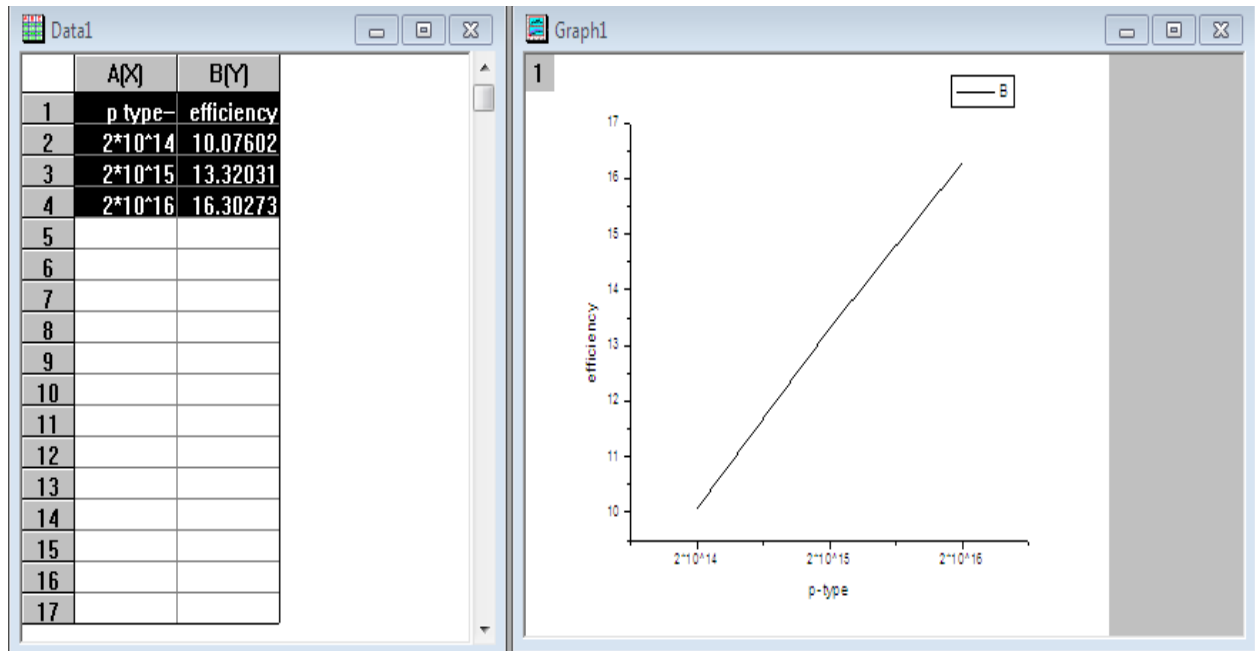|	A(X)	B(Y)
1	p type-	efficiency
2	2*10^14	10.07602
3	2*10^15	13.32031
4	2*10^16	16.30273

Fig: p-type vs efficiency

Chapter 4

Conclusion

In this experiment we have found that the efficiency of the solar cell increased by increasing the thickness and concentration of the BSF layer. There is also a significant effect of intrinsic layer. The effect of intrinsic layer thickness is linear with the efficiency of the solar cell. But there is also a fact that with the increased thickness of intrinsic layer we have to consider the price.

Our simulated results exhibit how the absorber and buffer layers thickness, defect density influence the short-circuit current density Isc is 34.235344 , open-circuit voltage Voc is 0.51, fill factor FF is 0.934, and efficiency (η) of solar cell. The optimized solar cell shows an efficiency of 16 % under the AM1.5G spectrum and one sun.

Reference

1. https://www.reference.com/science/definition-solar-energy-bd63bb5a85cb22a1

2. http://whatis.techtarget.com/definition/solar-power

3. https://www.reference.com/science/solar-energy-important-323345a2f5340b84

4. http://www.solartech-usa.com/types-of-solar-cells

5. http://www.jeos.org/index.php/jeos_rp/article/viewFile/14052/1278

6. https://www.irena.org/DocumentDownloads/Publications/RE_Technologies_Cost_Analysis-SOLAR_PV.pdf